

OFFICE OF NAVAL RESEARCH

Contract N00014-91-J-1641

R&T Code 313W001

TECHNICAL REPORT NO. 72

Influence of Surface Defects on Chlorine Chemisorption on Si(100)-(2 x 1)

by

W. Yang, Z. Dohnálek, W.J. Choyke and J.T. Yates, Jr.

Submitted To

Surface Science

Surface Science Center  
Department of Chemistry  
University of Pittsburgh  
Pittsburgh, PA 15260

12 June 1996

Reproduction in whole or in part is permitted for any  
purpose of the United States Government

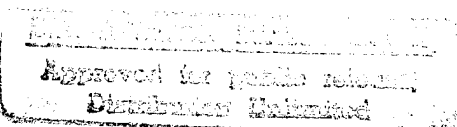
This document had been approved for public release and sale;  
its distribution is unlimited

19960701 086

## REPORT DOCUMENTATION PAGE

Form Approved  
OMB No. 0704-0188

Public reporting burden for this collection of information is estimated to average 1 hour per response, including the time for reviewing instructions, searching existing data sources, gathering and maintaining the data needed, and completing and reviewing the collection of information. Send comments regarding this burden estimate or any other aspect of the collection of information, including suggestions for reducing this burden, to Washington Headquarters Services, Directorate for Information Operations and Reports, 1215 Jefferson Davis Highway, Suite 1222, Arlington, VA 22202-4302, and to the Office of Management and Budget, Paperwork Reduction Project (0704-0188), Washington, DC 20585.

1. AGENCY USE ONLY (Leave blank)	2. REPORT DATE	3. REPORT TYPE AND DATES COVERED	
	June 12, 1996	Preprint	
4. TITLE AND SUBTITLE		5. FUNDING NUMBERS	
Influence of Surface Defects on Chlorine Chemisorption on Si(100)-(2 x 1)			
6. AUTHOR(S)			
W. Yang, Z. Dohnalek, W.J. Choyke and J.T. Yates, Jr.			
7. PERFORMING ORGANIZATION NAME(S) AND ADDRESS(ES)		8. PERFORMING ORGANIZATION REPORT NUMBER	
Surface Science Center Department of Chemistry University of Pittsburgh Pittsburgh PA 15260			
9. SPONSORING/MONITORING AGENCY NAME(S) AND ADDRESS(ES)		10. SPONSORING/MONITORING AGENCY REPORT NUMBER	
Office of Naval Research Chemistry Division Code 313 800 North Quincy Street Arlington, Virginia 22217-5000			
11. SUPPLEMENTARY NOTES			
12a. DISTRIBUTION / AVAILABILITY STATEMENT		12b. DISTRIBUTION CODE	
			
13. ABSTRACT (Maximum 1000 words)			
<p>The influence on chlorine chemisorption of surface defects created by low fluence Ar<sup>+</sup> sputtering of the Si(100)-(2x1) surface has been studied. A distinctly different type of Cl bonding is observed on defect sites compared to Cl bonding on Si-Si dimers, as judged by electron stimulated desorption ion angular distribution (ESDIAD) measurements. On the ordered Si(100) surface only terminally bonded Si-Cl species are observed (producing four off-normal Cl<sup>+</sup> beams); on the disordered Si(100) surface an additional Cl<sup>+</sup> beam emitted in the normal direction is present at 120K. This Cl<sup>+</sup> beam is interpreted as a bridge bonded Cl species chemisorbed inside of the dimer vacancy defects. In SiCl<sub>2</sub> thermal desorption a new low temperature desorption channel is observed on disordered Si(100) surfaces indicating that defect sites enhance the rate of surface etching. In the range of Ar<sup>+</sup> fluences studied (0.2-5 monolayer) the Cl saturation coverage increases by as much as 30%, over that observed on non-defective Si(100)-(2x1).</p>			
14. SUBJECT TERMS		15. NUMBER OF PAGES	
Temperature Programmed Desorption			
Silicon (100)	Chlorine	Electron Stimulated	
Surface Defects	Chemisorption	Desorption Ion Angular	
Low Bombardment	Etching	Distribution	
16. PRICE CODE			
17. SECURITY CLASSIFICATION OF REPORT	18. SECURITY CLASSIFICATION OF THIS PAGE	19. SECURITY CLASSIFICATION OF ABSTRACT	20. LIMITATION OF ABSTRACT

Submitted to: Surface Science  
Date: 12 June 1996

**INFLUENCE OF SURFACE DEFECTS ON CHLORINE  
CHEMISORPTION ON Si(100)-(2 X 1)**

W. Yang,<sup>†</sup> Z. Dohnálek, W.J. Choyke<sup>†</sup> and J.T. Yates, Jr.

Surface Science Center  
Department of Chemistry  
University of Pittsburgh  
Pittsburgh, PA 15260

<sup>†</sup>Department of Physics  
University of Pittsburgh  
Pittsburgh, PA 15260

# INFLUENCE OF SURFACE DEFECTS ON CHLORINE CHEMISORPTION ON Si(100)-(2×1)

W. Yang,<sup>†</sup> Z. Dohnálek, W.J. Choyke<sup>†</sup> and J.T. Yates, Jr.

Surface Science Center  
University of Pittsburgh  
Pittsburgh, PA 15260

<sup>†</sup>Department of Physics  
University of Pittsburgh  
Pittsburgh, PA 15260

## Abstract

The influence on chlorine chemisorption of surface defects created by low fluence  $\text{Ar}^+$  sputtering of the Si(100)-(2×1) surface has been studied. A distinctly different type of Cl bonding is observed on defect sites compared to Cl bonding on Si-Si dimers, as judged by electron stimulated desorption ion angular distribution (ESDIAD) measurements. On the ordered Si(100) surface only terminally bonded Si-Cl species are observed (producing four off-normal  $\text{Cl}^+$  beams); on the disordered Si(100) surface an additional  $\text{Cl}^+$  beam emitted in the normal direction is present at 120K. This  $\text{Cl}^+$  beam is interpreted as a bridge bonded Cl species chemisorbed inside of the dimer vacancy defects. In  $\text{SiCl}_2$  thermal desorption a new low temperature desorption channel is observed on disordered Si(100) surfaces indicating that defect sites enhance the rate of surface etching. In the range of  $\text{Ar}^+$  fluences studied (0.2-5 monolayer) the Cl saturation coverage increases by as much as 30%, over that observed on non-defective Si(100)-(2x1).

## I. Introduction

The role of surface defect sites on silicon single crystal surfaces in governing surface reactivity forms a major thrust of modern surface science research using many different surface measurement methods. In the case of Si(100)-(2 x 1) the clean surface exhibits wide terraces which may be highly defect free, separated by single atomic height steps. The terraces adjacent to such steps exhibit orthogonal arrangements of silicon dimer rows, as observed by STM [1]. The low surface density point defect sites often observed by STM on the flat terraces fall into several categories, termed type A (single missing dimers), type B (two adjacent missing dimers), and type C (two adjacent half missing dimers) [2], as well as the step defect sites separating Si(100)-(2x1) terraces. The detailed origin of the point defects is controversial, although measured submonolayer coverages of metals such as Ni have been correlated to the surface density of missing dimers observed by STM [3-6].

Defects on silicon surfaces are of importance because of their influence on microelectronic device fabrication [7], silicon epitaxial growth [8,9], and surface reactivity and photoreactivity [10,11]. A variety of defect structures have been observed on Si(100) following low fluence ion bombardment [12-14], and it was shown that these structures may be annealed away at 1223 K, returning the surface to the ordered condition [12]. No studies of surface defect production involving

ion bombardment of Si(100) at 120 K have been reported, and the work described here employed such low temperature bombardment in order to capture and study defect sites as they are formed rather than after thermally induced changes have occurred.

In this paper we use controlled levels of  $\text{Ar}^+$  bombardment to produce defect sites. The properties of chemisorbed chlorine on the defective surface changes dramatically from that observed on the ordered surface, as seen by both ESDIAD (electron stimulated desorption ion angular distribution) [15], and by the thermal desorption of the major thermal etch product,  $\text{SiCl}_2$ .

## II. Experimental

The experiments were carried out in an ultrahigh vacuum chamber with a base pressure of  $3 \times 10^{-11}$  Torr, as described previously [16,17]. The system is equipped with a digital LEED/ESDIAD apparatus, a CMA Auger electron spectrometer, a line-of-sight, shielded and apertured mass spectrometer for temperature programmed desorption, a second open-ionizer mass spectrometer for uptake measurements during  $\text{Cl}_2$  adsorption, an ion gun for highly controlled ion bombardment, and an absolutely calibrated capillary array doser for controlled adsorption of  $\text{Cl}_2$  gas, minimizing the vacuum system exposure to this corrosive gas.

Si(100) crystals (Virginia Semiconductor, float zone growth, p-type, boron doped, 5-20 ohm cm) of 0.4 mm thickness were used in the present experiments. Rectangular slabs of dimension 23 x 12 mm<sup>2</sup> were cut from the wafer, ultrasonically rinsed in methyl alcohol (spectrophotometric grade), and then in deionized water (10<sup>18</sup> ohm cm). On the manipulator the crystal was clamped on its ends between silicon bars made of the same material, and these bars were clamped tightly between Ta (Goodfellow, 99.9 %) spring structures. This method was shown to produce very uniform resistive heating across the crystal and to lead to contamination free Si [18].

Temperatures were measured using a W5%Re/W26%Re thermocouple, protected by a thin Ta tube, and contacted with the top edge of the crystal by means of bending the assembly into a springy U-shaped structure [18]. This arrangement has been shown to prevent metal contamination of the Si(100) surface. The thermocouple reading was compared to the reading of an optical pyrometer (corrected for Si emissivity and window reflection at 650nm) and it was found that it is about 80 K low at 1400 K compared to the pyrometer [18].

For cleaning, the crystal was heated to 1400 K, followed by fast cooling (~ 20 K/s) to 973 K and slow cooling (~ 2 K/s) to 100 K. The defective crystal was prepared at 120 K by Ar<sup>+</sup> ion bombardment (400 eV, 60° incidence angle) with an Ar<sup>+</sup> fluence varying from approx. 0.2 ML to 5.1 ML (1 ML = 6.78 x 10<sup>14</sup> ions/cm<sup>2</sup>). Careful impurity studies of the Si(100) crystal showed that only carbon

was visible by AES, and the C(LMM)/Si(LVV) peak-to-peak intensity ratio was reduced to 0.1 %, near the detection limit. Care was taken in the preparation of the crystal and in its handling to avoid contamination, particularly by metals, using procedures devised in parallel STM investigations [6]. The normal (2 x 1) LEED pattern was always found on the clean crystal.

Chlorine gas (99.999%, Matheson) was purified by freeze-pump-thaw procedures and was transferred to the sample using the doser connected to a well conditioned gas line. Both gas uptake curves and Auger spectroscopy were used to ascertain the Cl coverage. The Cl(KLL)/Si(LVV) ratio was employed, using a 0.3  $\mu$ A electron beam current for <30 s measurement periods to avoid any significant electron stimulated desorption.

All ESDIAD data were collected at a crystal temperature of 100 K with a primary electron energy of 120 eV at a collected current of < 10nA. The incidence angle was 45°. The potentials within the apparatus were:  $V_{\text{crystal}} = +15$  V; the grid potential  $V_{G1} = V_{G2} = V_{G3} = 0$  V;  $V_{G4} = +14$  V; and  $V_{G5} = - 500$  V, where the five grids are numbered in accordance with their distance from the crystal. The ESDIAD patterns were corrected for the soft X-ray background effect measured [19], and were smoothed by a 5-point smoothing routine [20]. The integrated volume of the ESDIAD pattern was used to evaluate the relative  $\text{Cl}^+$  ESD yield.

### III. Results

#### A. ESDIAD Measurements on Ordered and Disordered Si(100)

Figure 1a shows the  $\text{Cl}^+$  ESDIAD pattern produced by partial monolayer adsorption of  $\text{Cl}_2$  on an ordered  $\text{Si}(100) - (2 \times 1)$  surface at 100 K. Four sharp  $\text{Cl}^+$  beams, oriented in the  $\langle 011 \rangle$  and  $\langle 01\bar{1} \rangle$  directions can be observed, and correspond to the Si-Cl bonds originating from the Si dangling bonds associated with the orthogonal sets of dimer sites present on the surface [21,22]. Upon annealing the surface to 673 K, and then cooling back to 100 K, the slightly intensified four beam pattern shown in Figure 1b is observed.

Figure 2a shows an identical adsorption experiment performed at 100 K on a defective surface produced by 1.9 ML  $\text{Ar}^+$  bombardment at 120 K. The  $\text{Cl}^+$  ESDIAD pattern is quite different from that observed on the ordered surface, and is characterized by a sharp normal  $\text{Cl}^+$  beam having only a slight hint of the four-fold symmetry which was seen on the ordered surface. Upon annealing the surface containing the chemisorbed Cl to 673 K, the four beam pattern is regenerated (Figure 2b) without substantial loss in intensity compared to the control experiment on the ordered surface shown in Figure 1b.

Figure 3 shows the profiles of the  $\text{Cl}^+$  ESDIAD patterns obtained for varying levels of defect production by  $\text{Ar}^+$  bombardment prior to  $\text{Cl}_2$  adsorption to saturation coverage. The relative and absolute intensity of the normal  $\text{Cl}^+$  component of the ESDIAD pattern systematically increases as the degree of defect production is increased by increased ion bombardment. In addition, the total yield of  $\text{Cl}^+$  monotonically increases as the damage by  $\text{Ar}^+$  bombardment is increased up to 5 ML of  $\text{Ar}^+$ .

The enhanced yield of  $\text{Cl}^+$  as the level of surface damage increases is indicative of the presence of an increasing surface density of defect sites. These defect sites may be removed by annealing, and this is reflected in a decrease in the saturation-coverage  $\text{Cl}^+$  yield, as shown in Figure 4. In Figure 4, a 1.9 ML dose of  $\text{Ar}^+$  was used to initially disorder the surface at 120 K. Following this, various annealing temperatures were employed, followed by saturation  $\text{Cl}_2$  adsorption. A sharp decrease in the  $\text{Cl}^+$  yield is observed for annealing above about 300 K, and the effect culminates at about 700 K. The reduction in  $\text{Cl}^+$  yield to near zero in these experiments is due to self quenching effects between neighboring Cl atoms at the high coverages achieved here [23]. This quenching effect between neighboring Cl atoms decreases significantly when the surface contains point defects made by  $\text{Ar}^+$  bombardment. Because of the strong self-quenching on an ordered Si(100) surface, the production of four  $\text{Cl}^+$  ESDIAD beams upon

annealing to 673 K, as shown in Figure 2, was intentionally measured at lower Cl coverages where this quenching effect was not dominant.

### **B. Temperature Programmed Desorption Studies**

Temperature programmed desorption of Cl/Si(100) layers results in  $\text{SiCl}_2$  desorption near 960 K from the ordered surface. For disordered Si(100), Figure 5 indicates that additional desorption of  $\text{SiCl}_2$  occurs near 600 K, and that the relative quantity of this low temperature desorption product increases as the level of surface damage, prior to  $\text{Cl}_2$  adsorption, increases. In addition to this effect, the desorption peak shape for the high temperature  $\text{SiCl}_2$  desorption process changes from a sharp, high temperature peak on the undamaged surface, to a broader and somewhat lower temperature peak on the damaged surface. Annealing the highly damaged surface to 673 K begins to reverse these two effects as surface ordering of Si(100) begins to occur (Fig. 5e), and annealing to 1400 K returns the surface to an ordered condition as shown in initial TPD spectrum (Fig. 5a).

### **C. Auger Spectroscopy Studies of Cl Surface Coverage**

Figure 6 shows results from Auger spectroscopy studies of the saturation coverage of Cl on Si(100) which has been damaged to various levels by  $\text{Ar}^+$

bombardment. In addition, the effect of annealing the saturated layer to 673 K is shown at the various levels of initial damage. Two effects are evident: (1) For the damaged surface, the saturation Cl coverage rises significantly in the first 0.5 ML  $\text{Ar}^+$  damage regime, and then rises more slowly at higher damage levels; (2) Annealing the Cl-saturated  $\text{Si}(100)$  to 673 K removes Cl by amounts of  $\sim 30\%$  or less, depending on the initial damage level. For annealing experiments on surfaces with zero or low damage levels, little decrease in the Cl coverage occurs on annealing to 673 K. These results are qualitatively in agreement with the TPD experiments shown in Figure 5, where the presence of surface defects produced by  $\text{Ar}^+$  bombardment provides a low temperature desorption channel releasing  $\text{SiCl}_2$  below 673 K.

#### IV. Discussion

Three separate effects are observed to occur in the behavior of adsorbed Cl when defect sites are introduced on  $\text{Si}(100)-(2 \times 1)$  by  $\text{Ar}^+$  bombardment. These are:

- (1) The production of a normal  $\text{Cl}^+$  ESDIAD beam;
- (2) The increase of a saturation chlorine coverage;
- (3) The formation of a low temperature  $\text{SiCl}_2$  thermal desorption state.

In this section we propose possible mechanisms leading to the above mentioned effects.

#### A. Origin of Normal Cl<sup>+</sup> ESDIAD Pattern on Si Defect Sites

Figure 7a shows a single silicon dimer vacancy defect site which might be produced by Ar<sup>+</sup> bombardment. Remaining on this site are four inclined Si dangling bonds located on the second layer Si atoms, and inclined towards each other. The dimer vacancy has been observed by STM when defect sites are produced by sputtering [12-14], by the introduction of Ni impurity atoms [4-6], and by thermal etching of Si(100) as SiCl<sub>2</sub> species are desorbed from the surface [24].

We postulate that the adsorption of two symmetrically bridged Cl species on the dimer defect sites is possible (Figure 7) and these symmetric species will yield a normal Cl<sup>+</sup> ESDIAD beam. Species of this type were detected earlier by HREELS studies on Si(100) surfaces now known to possess defect site coverages in excess of those now present on our clean, low defect level Si(100) surfaces. These sites yield bridged Cl species exhibiting a stretching frequency of 300 cm<sup>-1</sup>, and this vibrational mode disappears when the Cl-covered surface is annealed to about 673 K [21]. These symmetrically bound Cl species would be expected to desorb in ESDIAD normally from the surface since the resultant repulsive vector

force on the desorbing  $\text{Cl}^+$  will be in the normal direction for the symmetrical structure.

### **B. Enhanced Cl Coverage on Defective Si(100)**

Figure 6 shows that as much as 30 % enhancement in the saturation coverage of Cl can exist on highly defective Si(100) initially subjected to heavy (5ML) ion bombardment damage. This comparison is made to the surface after annealing to 673 K, where  $\text{SiCl}_2$  in the defect-related low temperature desorption channel has been evolved, as shown in Figure 5. Our model, involving the bridging Cl species on the single dimer vacancy sites, would not be expected to yield enhanced Cl coverage, since two Si-Cl species present on the ordered dimer site are replaced by two bridged Si-Cl-Si species on the single dimer vacancy site as may be seen by examination of Figure 7b. However, it is known that dimer vacancies can cluster, as shown in Figure 8, and under these conditions a mixture of Si-Cl species and  $\text{SiCl}_2$  surface species may be produced on the defect site, leading to the adsorption of excess Cl compared to the perfect surface.

### **C. Low Temperature $\text{SiCl}_2$ Desorption from Vacancy Defect Sites**

Figure 5 shows the development of the low temperature  $\text{SiCl}_2$  desorption state as the  $\text{Ar}^+$  damage level is increased. The formation of  $\text{SiCl}_2$  as a volatile

product indicates that at desorption temperature, Si-Si back bonds are being broken, and Si-Cl bonds are formed as etching occurs. These processes can easily be visualized on the dimer vacancy defect sites where exposure of second and third level Si atoms to Cl occurs, and where in the case of clusters of Si dimer defects (Figure 8), surface  $\text{SiCl}_2$  species may be formed upon adsorption on a second layer Si atom which has lost its coordination to two of its four original Si neighbors.

#### **D. Connection to Other Studies**

Although not shown in this work, heating of a Cl-saturated Si(100) surface to 873 K also produces an ESDIAD pattern containing mainly normal  $\text{Cl}^+$  emission, indicative of dimer vacancy defect sites produced by etching through  $\text{SiCl}_2$  desorption in the high temperature state [21]. Furthermore, in a companion paper [25], the use of small amounts of impurity Ni, to produce split-off dimer structures, and other dimer vacancy structures has been studied. Ni-induced dimer vacancies are also associated with a normal  $\text{Cl}^+$  ESDIAD beam, with enhanced Cl coverage, and with the low temperature  $\text{SiCl}_2$  desorption process.

Annealing to 673 K seems to remove the majority of the dimer vacancy defect sites responsible for the effects studied here, although annealing to 1400 K

is needed to bring the surface back to the starting condition in which the low temperature  $\text{SiCl}_2$  production is diminished to its lowest level (Figure 5).

## V. Conclusions

Three unique observations related to Cl chemisorption on  $\text{Si}(100)$ , which contains defect sites produced by low fluence 400 eV  $\text{Ar}^+$  damage, have been made, using ESDIAD, Cl coverage measurements, and the thermal desorption of the etch product,  $\text{SiCl}_2$ . These are:

1. Vacancy defect sites are associated with the production of a normal  $\text{Cl}^+$  ESDIAD beam which differs from the tilted Si-Cl beams associated with Cl chemisorption on the dangling bonds of normal surface Si dimer sites. The presence of the normal  $\text{Cl}^+$  ESDIAD beam provides an extremely sensitive method for defect site detection.
2. An enhancement of Cl surface coverage up to an extra 30% occurs on heavily damaged  $\text{Si}(100)$  surfaces as Si-Si back bonds become accessible.
3. The desorption of  $\text{SiCl}_2$  in a low temperature process near 600 K is characteristic of the presence of vacancy defect sites.

Rationalizations of all three of these experimental observations have been made based on the assumption that sputtering at 120 K results in the production of

dimer vacancy defect sites, and that clustering of these sites can occur at higher temperatures. The vacancy defect sites detected by these three experimental observations begin to be removed by annealing the damaged Si(100) surface to 673 K.

## VI. Acknowledgments

We thank the Office of Naval Research for support of this work. One of us (WY) acknowledges the International Union of Vacuum Science and Technology for the Award of a Welch Scholarship. Another (ZD) acknowledges the receipt of a Lubrizol Student Fellowship.

## References:

- [1] Hanne Neergaard Waltenburg and John T. Yates, Jr., *Chem. Rev.* **95** (1995) 1589.
- [2] R.J. Hamers and U.K. Köhler, *J. Vac. Sci. Technol. A7* (1989) 2854.
- [3] K. Kato, T. Ide, S. Miura, A. Tamura and T. Ichinokawa, *Surf. Sci.* **194** (1988) L87.
- [4] H.J.W. Zandvliet, H.K. Louwsma, P.E. Hegeman and B. Poelsema, *Phys. Rev. Lett.* **75** (1995) 3890.
- [5] H. Niehus, U.K. Köhler, M. Copel and J.E. Demuth, *J. Microscopy*, **152** (1988) 735.
- [6] V. A. Ukrainstev and J. T. Yates, Jr., *Surf. Sci.* **346** (1996) 31.
- [7] K.V. Ravi, *Imperfections and Impurities in Semiconductor Silicon* (Wiley, New York, 1981).
- [8] B.S. Swartzentruber, C.M. Matzke, D.L. Kendall and J.E. Houston, *Surf. Sci.* **329** (1995) 83.
- [9] M.V. Ramana Murty and H.A. Atwater, *Phys. Rev B45* (1992), 1507.
- [10] M.J.Bozack, W.J. Choyke, L. Muehlhoff and J.T. Yates, Jr., *Surf. Sci.* **176** (1986) 547.
- [11] P.M. Chu, S. A. Buntin, L.J.Richter, R.R. Cavanagh, *Surf. Sci.* **321** (1994) 127.
- [12] H. Feil, H.J.W. Zandvliet, M.-H. Tsai, J.D. Dow and I.S.T. Tsong, *Phys. Rev. Lett.* **69** (1992) 3076.
- [13] H.J.W. Zandvliet, H.B. Elswijk and E.J. van Loenen, *Phys. Rev. B* **46** (1992) 7581.
- [14] P. Bedrossian, *Surf. Sci.* **301** (1994) 223.

[15] R.D. Ramsier and J.T. Yates, Jr., *Surf. Sci. Reports* **12** (1991) 243. J.T. Yates, Jr., M.D. Alvey, M.J. Dresser, M.A. Henderson, M. Kiskinova, R.D. Ramsier and A. Szabó, *Science*, **255** (1992) 1397.

[16] M.J. Bozack, L. Muehlhoff, J.N. Russell,Jr., W.J. Choyke and J.T. Yates, Jr., *J. Vac. Sci. Technol. A* **5** (1987) 1.

[17] R.M. Wallace, P.A. Taylor, W.J. Choyke and J.T. Yates, Jr., *Surf. Sci.* **239** (1990) 1.

[18] H. Nishino, W. Yang, Z. Dohnalek, V. A. Ukrainstev and J. T. Yates, Jr., submitted to *J. Vac. Sci. Technol. A*.

[19] M.J. Dresser, M.D. Alvey and J.T. Yates.Jr., *Surf. Sci.* **169** (1986) 91.

[20] A. Szabó, M. Kiskinova and J.T. Yates, Jr., *Surf. Sci.* **205** (1988) 207.

[21] Q. Gao, C. C. Cheng, P. J. Chen, W. J. Choyke and J. T. Yates, Jr. *J. Chem. Phys.* **98** (1993) 8308.

[22] C. C. Cheng, Q, Gao, W. J. Choyke and J. T. Yates, Jr. *Phys. Rev B* **46** (1992), 12810.

[23] E.B. Stechel, M.L. Knotek, *Surf. Sci.* **167** (1986) 297.

[24] M. Chander, D.A. Goetsch, C.M. Aldao and J.W. Weaver, *Phys. Rev. Lett.* **74** (1995) 2014.

[25] Z. Dohnálek, W. Yang, V. A. Ukrainstev, W.J. Choyke and J.T. Yates, Jr., following paper.

## Figure Captions

**Figure 1.** (a)  $\text{Cl}^+$  ESDIAD patterns following  $\text{Cl}_2$  adsorption ( $\text{Cl}_{(\text{KLL})}/\text{Si}_{(\text{LVV})}=0.24$ ) on the  $\text{Si}(100)-(2\times 1)$  surface at 120K; (b) subsequent annealing at 673K (b). The patterns are presented as 2-dimensional contour plots and as 3-dimensional plots

**Figure 2.** (a)  $\text{Cl}^+$  ESDIAD patterns following the dose of  $\text{Si}(100)$  surface by 1.9ML of  $\text{Ar}^+$  ions ( $E_{\text{Ar}^+} = 400\text{eV}$ , angle of incidence =  $60^\circ$ ) and  $\text{Cl}_2$  adsorption ( $\text{Cl}_{(\text{KLL})}/\text{Si}_{(\text{LVV})}=0.24$ ) at 120K; (b) subsequent annealing at 673K. The patterns are presented as 2-dimensional contour plots and 3-dimensional plots

**Figure 3.** 2-dimensional profiles taken from the original  $\text{Cl}^+$  ESDIAD patterns in the  $\langle 011 \rangle$  direction as a function of increasing  $\text{Ar}^+$  dose. All profiles are obtained after  $\text{Cl}_2$  saturation of  $\text{Ar}^+$  dosed  $\text{Si}(100)$  surfaces at 120K.

**Figure 4.** The effect of annealing of the disordered  $\text{Si}(100)$  surface ( $\text{Ar}^+$  dose = 1.9ML at 120K) on the total  $\text{Cl}^+$  ESDIAD yield. The  $\text{Si}(100)$  surfaces were saturated by  $\text{Cl}_2$  at 120K after the surface annealing.

**Figure 5.**  $\text{SiCl}^+$  TPD spectra from  $\text{Cl}_2$  saturated  $\text{Si}(100)$  surface for: (a) ordered surface; (b) - (d) disordered surfaces produced by 0.2ML, 0.9ML, and 1.9ML of

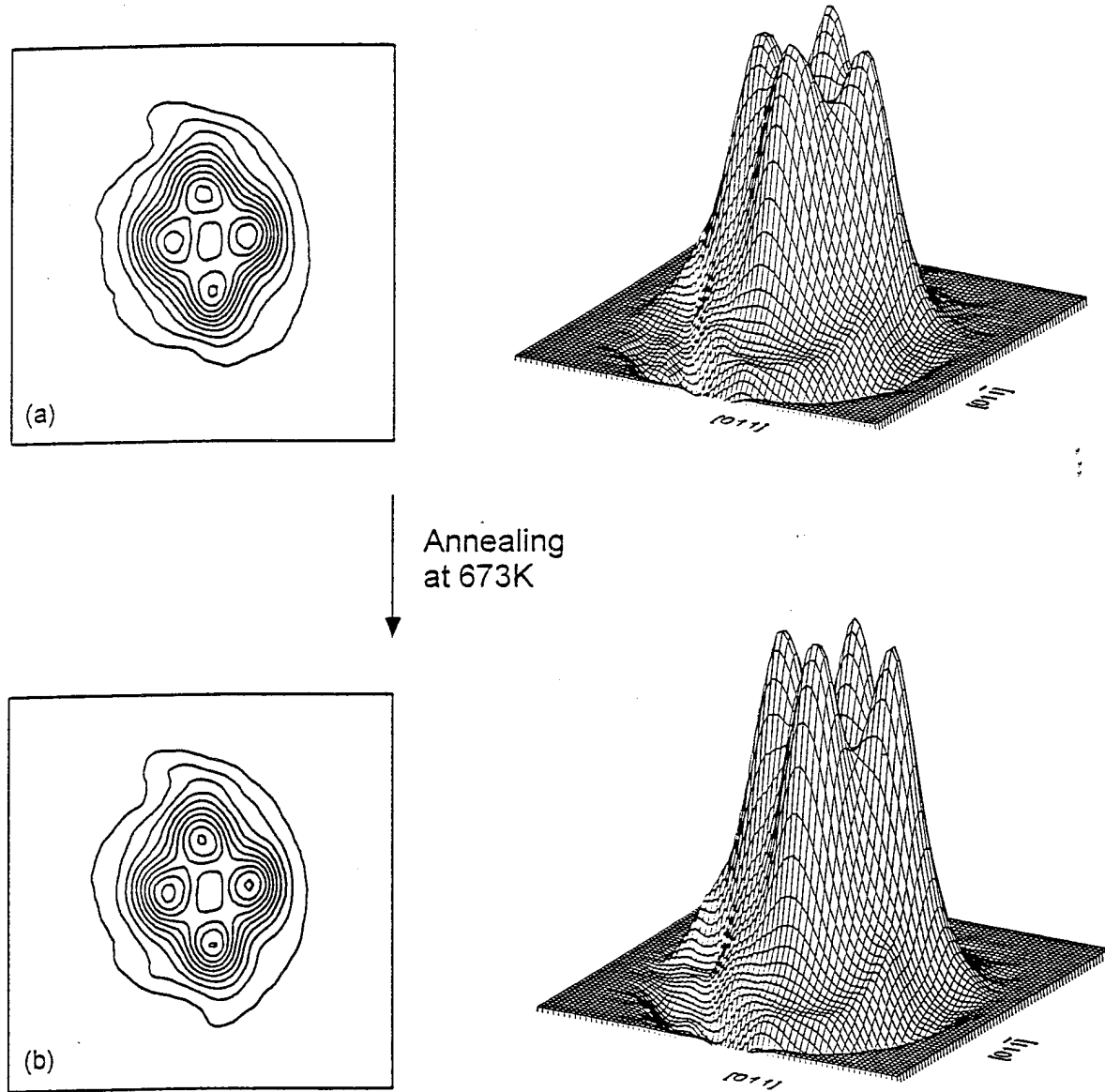
$\text{Ar}^+$  ions, respectively; (c) disordered surface exposed to 1.9ML of  $\text{Ar}^+$  ions followed by annealing at 673K. All spectra were acquired with a temperature ramp of 3K/s.

**Figure 6.** The  $\text{Cl}_{(\text{KLL})}/\text{Si}_{(\text{LVV})}$  Auger peak ratio for  $\text{Cl}_2$  saturated  $\text{Si}(100)$  surfaces as a function of increasing exposure to  $\text{Ar}^+$  ions: (a) after saturation at 120K; (b) subsequent annealing at 673K.

**Figure 7.** A schematic top view of a Si-Si dimer row showing a model for: (a) single dimer vacancy defect on the  $\text{Si}(100)$  surface; (b) single vacancy dimer defect saturated by chlorine bridge bonded species, and a proposed model of normal  $\text{Cl}^+$  ion production from such a species.

**Figure 8.** A schematic top view of a Si-Si dimer row showing a model for a double dimer vacancy defect on  $\text{Si}(100)$  surface saturated by chlorine species.

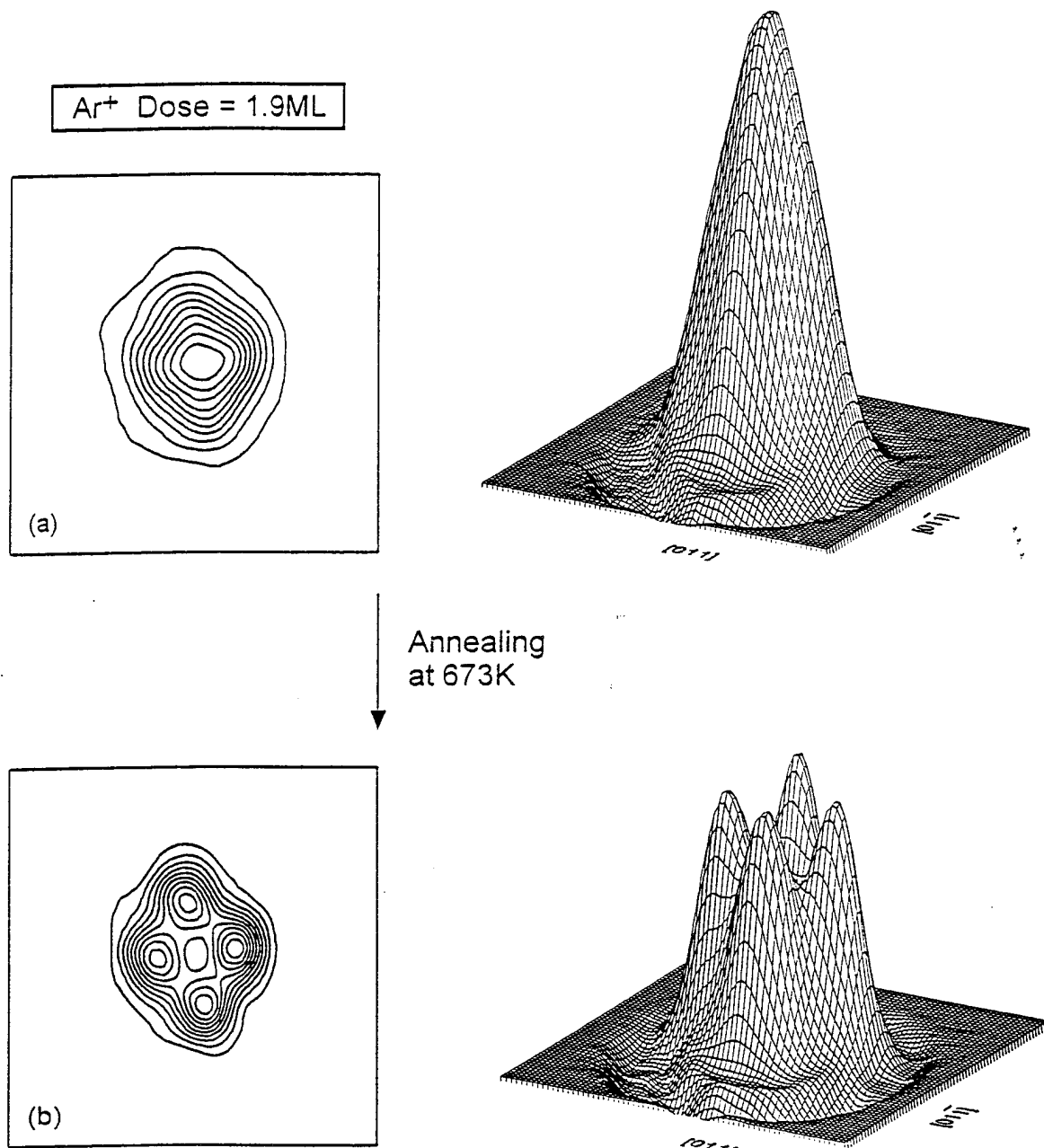
# Cl<sup>+</sup> ESDIAD Patterns from Ordered Si(100) Surface



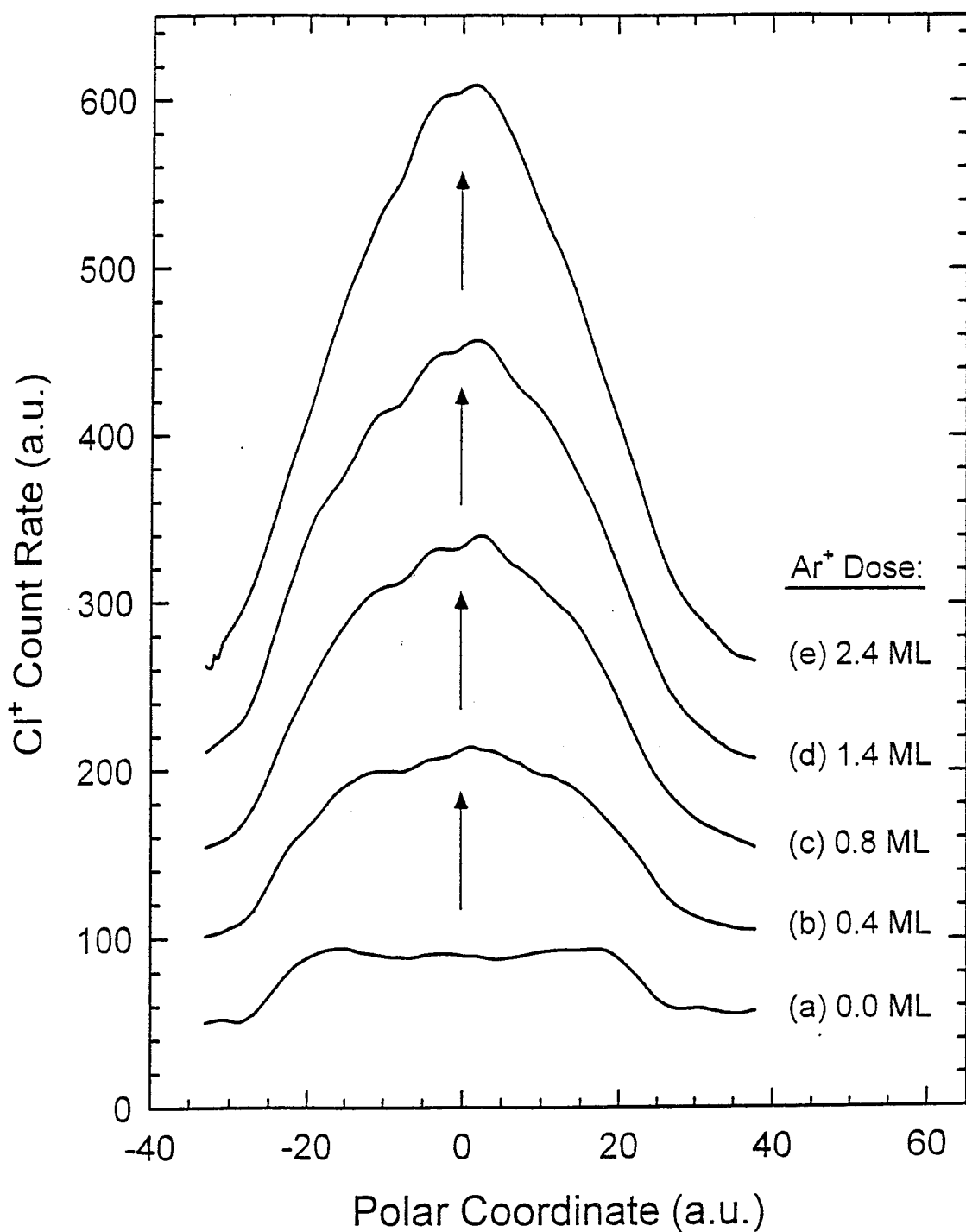
Yang, et al.

Figure 1

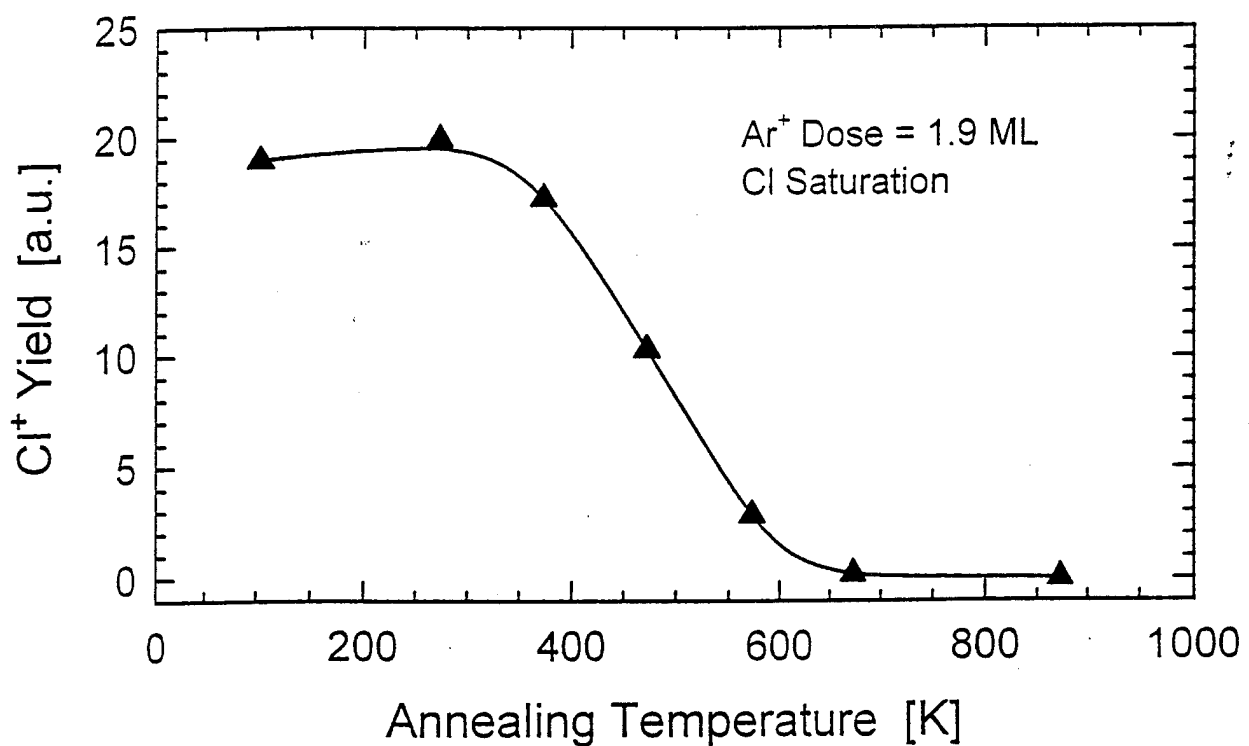
# Cl<sup>+</sup> ESDIAD Patterns from Disordered Si(100) Surface



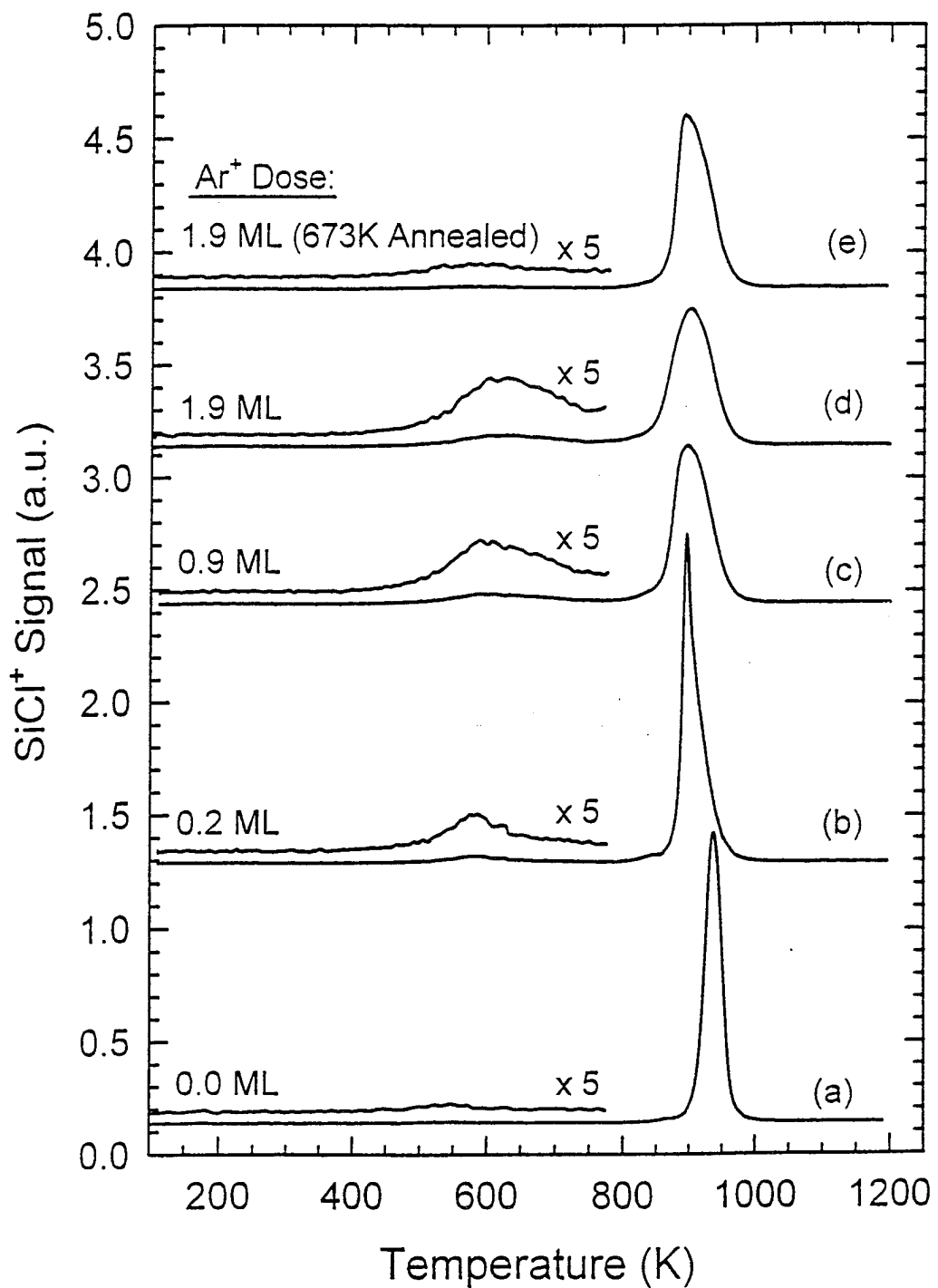
## Cl<sup>+</sup> ESDIAD Patterns for Various Ar<sup>+</sup> Damage Levels



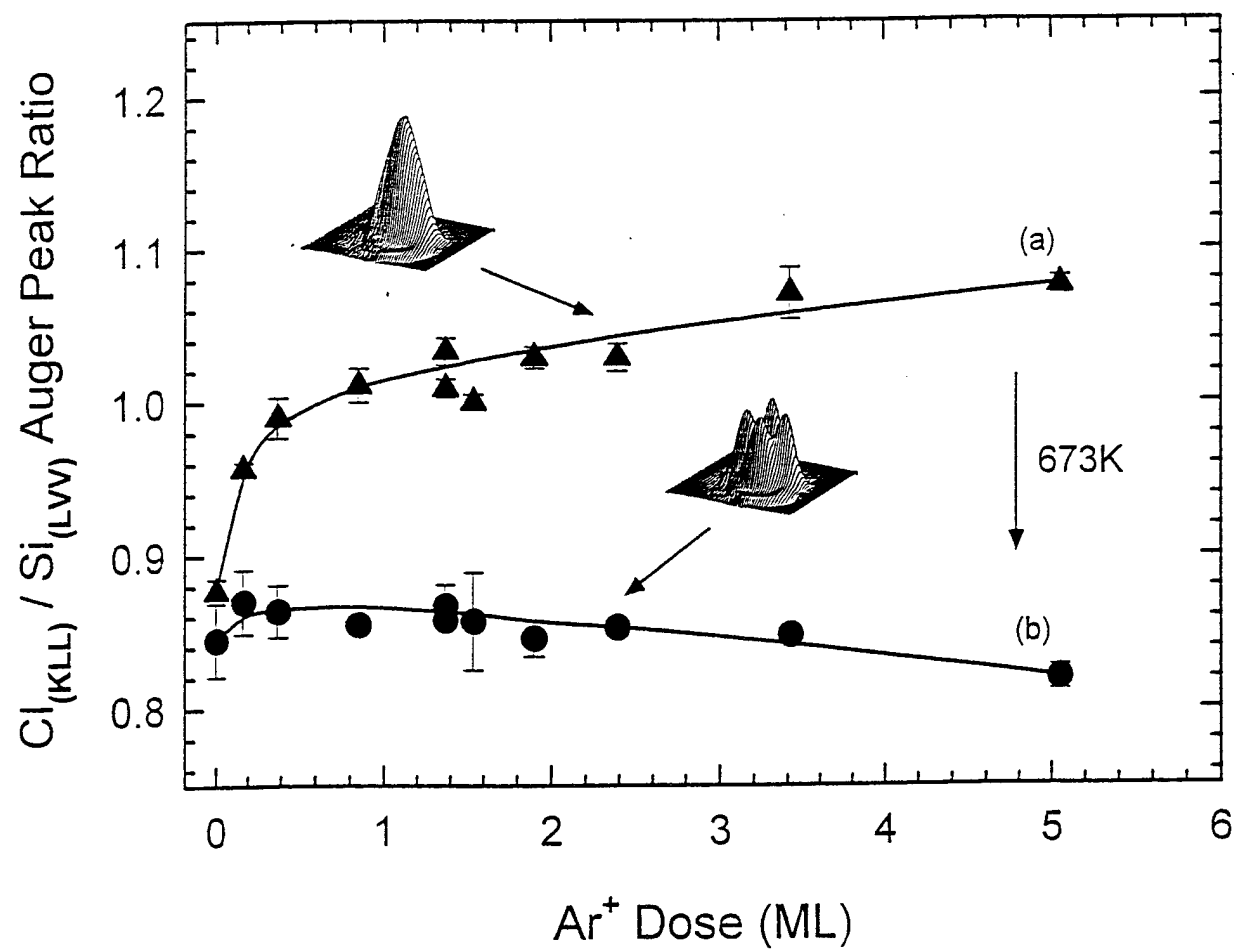
Effect of Annealing of Disordered Si(100) Surface  
Followed by Saturation with  $\text{Cl}_2$  at 120K



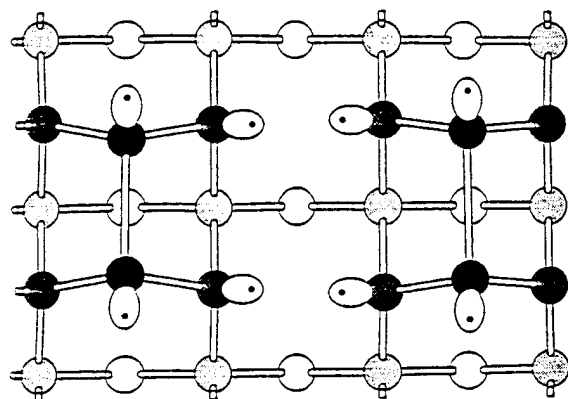
Thermal Desorption of  $\text{SiCl}_2$  Following Adsorption of  $\text{Cl}_2$  on Ordered and Defective Si(100)



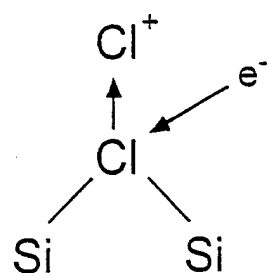
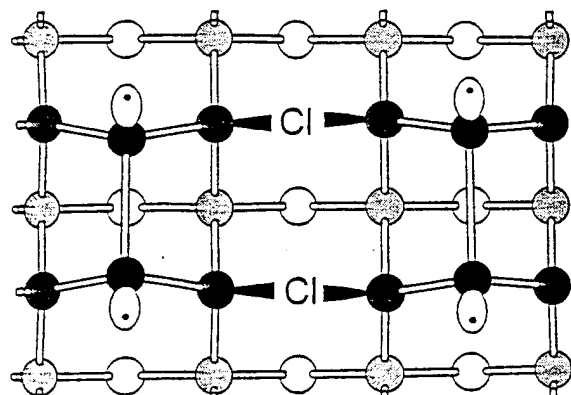
Cl<sub>(a)</sub> Saturation Coverage and Coverage Change  
After 673K Annealing as a Function of Ar<sup>+</sup> Dose



## Single Dimer Vacancy Defect on Si(100) and Bridging Cl in Vacancy

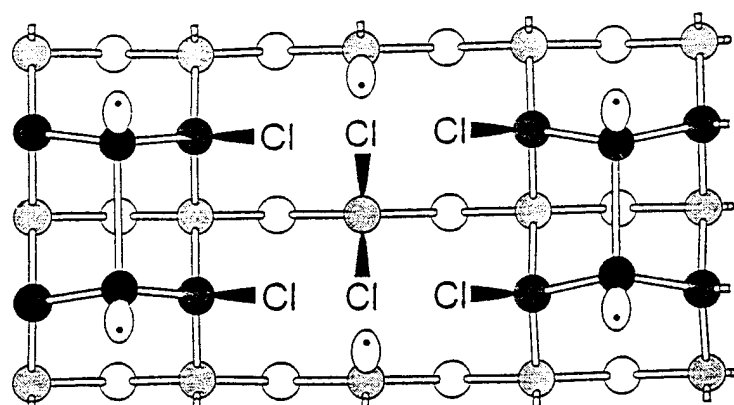


(a) Single dimer vacancy defect on Si(100)



(b) Bridging Cl in single dimer vacancy defect

Double Vacancy Cluster Saturated with Cl  
to form  $\text{SiCl}$  and  $\text{SiCl}_2$  Species



Dr. John C. Pazik (1)\*  
Physical S&T Division - ONR 331  
Office of Naval Research  
800 N. Quincy St.  
Arlington, VA 22217-5660

Defense Technical Information Ctr (2)  
Building 5, Cameron Station  
Alexandria, VA 22314

Dr. James S. Murday (1)  
Chemistry Division, NRL 6100  
Naval Research Laboratory  
Washington, DC 20375-5660

Dr. John Fischer (1)  
Chemistry Division, Code 385  
NAWCWD - China Lake  
China Lake, CA 93555-6001

Dr. Peter Seligman (1)  
NCCOSC - NRAD  
San Diego, CA 92152-5000

Dr. Bernard E. Douda (1)  
Crane Division  
NAWC  
Crane, Indiana 47522-5000

\* Number of copies required